



## Platinum zone plates for hard X-ray applications

E. Chubarova<sup>a</sup>, D. Nilsson<sup>a</sup>, M. Lindblom<sup>a</sup>, J. Reinspach<sup>a</sup>, J. Birch<sup>b</sup>, U. Vogt<sup>a</sup>, H.M. Hertz<sup>a</sup>, A. Holmberg<sup>a,\*</sup>

<sup>a</sup>Biomedical and X-Ray Physics, Department of Applied Physics, Royal Institute of Technology (KTH), Stockholm SE-106 91, Sweden

<sup>b</sup>Thin Film Physics, Department of Physics, Chemistry, and Biology, Linköping University, SE-581 83, Sweden

### ARTICLE INFO

#### Article history:

Received 18 January 2011

Received in revised form 17 May 2011

Accepted 20 June 2011

Available online 26 June 2011

#### Keywords:

Zone plate

Pt electroplating

X-ray optics

Electron beam lithography

### ABSTRACT

We describe the fabrication and evaluation of platinum zone plates for 5–12 kV X-ray imaging and focusing. These nano-scale circular periodic structures are fabricated by filling an e-beam generated mold with Pt in an electroplating process. The plating recipe is described. The resulting zone plates, having outer zone widths of 100 and 50 nm, show good uniformity and high aspect ratio. Their diffraction efficiencies are 50–70% of the theoretical, as measured at the European Synchrotron Radiation Facility. Platinum shows promise to become an attractive alternative to present hard X-ray zone plate materials due to its nano-structuring properties and the potential for zone-plate operation at higher temperatures.

© 2011 Elsevier B.V. All rights reserved.

### 1. Introduction

Nanometer X-ray focusing and imaging is of growing importance, at synchrotrons as well as with laboratory systems [1]. Zone plates are often the preferred high-resolution X-ray optical element in such microscopy systems, both in the water window (approx. 0.3–0.5 keV) and in the hard X-ray regime (up to ~12 keV). The fabrication of such lenses presently relies on a limited number of materials having the necessary combination of appropriate X-ray optical constants and process parameters which allow nano-scale fabrication. In the present paper we introduce a new material, platinum, for zone plates, describe its fabrication and demonstrate its applicability for the hard X-ray range.

Zone plates are circular diffraction gratings with radially decreasing line width. Their imaging properties are determined by two characteristics: the outermost zone width,  $dr_N$ , which sets the resolution, and the optical material and its thickness, which determines the diffraction efficiency [2]. Zone plates for the hard X-ray regime typically employ heavy metals as the optical material. Presently zone plates have been demonstrated in Ta [3], W [4], Ir [5,6] and Au [7]. Fig. 1 depicts the theoretically calculated efficiency at 8 kV as a function of material thickness for these materials and Pt. Clearly a high thickness is important for high diffraction efficiency and thus, a high aspect ratio becomes necessary for operation at high-resolution. In brief, three fabrication methods are used for patterning the metal, dry etching via a hard mask (Ta and W), atomic layer deposition on a mold (Ir) and electroplating

in a polymer mold (Au). The dry etching processes have typically demonstrated 50–100 nm outer zone width, with aspect ratios up to 12, while the atomic layer deposition of Ir presently allows <15 nm and an aspect ratio of 25 due to the line doubling effect. For the electroplating process, present state-of-the-art hard X-ray gold zone plates have an outer zone width of 24 nm and a thickness of 300 nm [7]. For comparison, electroplated zone plates for the soft X-ray range are best made of nickel, presently allowing 13 nm outer zone width and 35 nm height [8].

The diverse fabrication methods and material choices that have been used so far is a consequence of the quest for optics with higher resolution and improved diffraction efficiency. Pt is a high-Z metal optical material that has not been investigated previously. Although the efficiency for Pt is similar to the other materials (cf. Fig. 1), it has other properties that make it interesting for zone plate fabrication. First, Pt can be electroplated and is therefore suitable for similar processes as Au. Second, when comparing to Au, the melting point of Pt is 2045 K as compared to the melting point of Au at 1338 K. This would potentially allow operation at higher temperatures, something that is of growing importance with the emergence of high-power, high-brilliance 4th generation hard X-ray synchrotron sources [9]. Third, the sputter etch resistance of Pt is 2× that of Au, which can make it suitable for “multi-material” zone plates. We have recently fabricated multi material zone plates for soft X-ray applications [10]. Here an electroplated Ni zone plate was used as mask for extending the pattern into a thick Ge layer by dry etching, thereby doubling the efficiency compared to the original Ni zone plate. Pt has potential to be a very good electroplated mask material for a similar process in the hard X-ray optics. Finally, Pt is also an interesting material for dry etching. It forms

\* Corresponding author.

E-mail address: [anders.holmberg@bio.kth.se](mailto:anders.holmberg@bio.kth.se) (A. Holmberg).

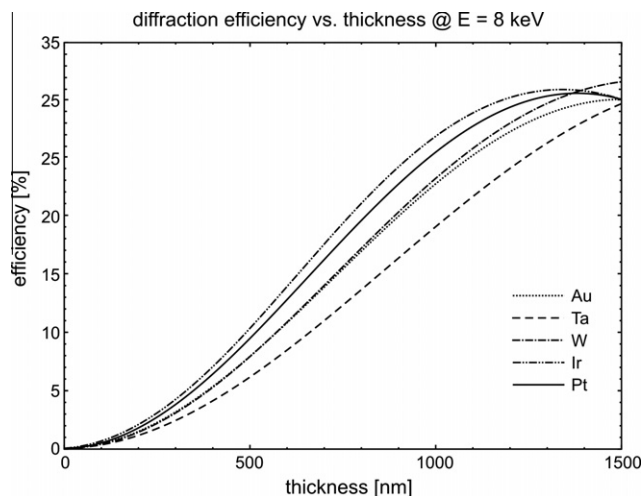


Fig. 1. Theoretical efficiency of hard X-ray zone plates at 8 kV for different heavy-metal elements.

the volatile compound  $\text{PtF}_6$  with a boiling point of  $69^\circ\text{C}$  (NTP), which makes it suitable for standard F-based dry etching. It could therefore be interesting for new multi-material approaches as a metal for dry etching. Thus, Pt appears to have a large potential as a future hard X-ray optical material.

In the present paper we demonstrate the fabrication of Pt zone plates down to 50 nm outer zone width and with high efficiency using electroplating. We note that although Pt electroplating is commonly used in a wide range of industrial coating applications [11,12] the Pt plating of repetitive high-aspect-ratio nanostructures with <100 nm dimensions have not been achieved before. Single platinum nanowires have been made using photolithography patterning followed by platinum electrodeposition [13] or by electrochemical fountain pen nanofabrication [14]. Platinum nano-hole-arrayed electrodes have been synthesized by template wetting [15]. Micro structured electro-plated Pt has been used for biomedical and other applications [16,17].

## 2. Experimental methods

### 2.1. Nanofabrication process

The fabrication of the platinum zone plate is based on the process depicted in Fig. 2. This process is suitable for high aspect-ratio periodic structures like zone plates, gratings and test structures [18]. In brief, the structures are made by electroplating platinum into a polymer mold made out from a tri-layer resist that is structured by electron beam lithography (EBL) and reactive ion etching (RIE).

Fifty nanometers silicon nitride membranes were used as substrates and coated with a stack of materials (Fig. 2a). First, a plating base was deposited by electron-beam evaporation (Edwards Auto 306 system,  $10^{-6}$  Torr base pressure). It consists of a 20 nm adhesive layer of titanium covered by a 30 nm plating seed layer of gold. Then the trilayer resist consisting of 550 nm thick polyimide as plating-mold (PI-2610, HD Microsystems), a 50 nm  $\text{SiO}_2$  hard mask and a 110 nm thick electron-beam resist (Zep 7000, Nippon Zeon Co.) was deposited. The polyimide and the electron-beam resist were spun cast and baked at  $350^\circ\text{C}$  for 2.5 h and at  $170^\circ\text{C}$  for 30 min, respectively. The  $\text{SiO}_2$  hard mask was sputter deposited (AJA Orion,  $10^{-8}$  Torr base pressure) at 3 mTorr pressure, 25 sccm Ar flow, and 100 W power.

The samples were patterned by EBL at 25 keV (Raith 150 system), with a typical dose of  $150 \mu\text{C}/\text{cm}^2$ , and developed in hexyl acetate for 30 s (Fig. 2b). The pattern was transferred into  $\text{SiO}_2$  hard mask using RIE with  $\text{CHF}_3$  (Oxford Instruments, Plasmalab 100) at 10 sccm flow, 3 mTorr pressure and 100 W power (Fig. 2c). The selectivity between  $\text{SiO}_2$  hard mask and electron-beam resist upon these conditions is 1:1. 25 nm wide lines are clearly resolved in such a processing. Then the pattern was transferred into the underlying polyimide layer by RIE with  $\text{O}_2$  (Oxford Instruments, Plasmalab 80+) at 10 sccm flow, 2 mTorr pressure and 50 W power resulting in the plating mold (Fig. 2d). At the next step of the process the platinum was electroplated into the mold (Fig. 2e). The electroplating of platinum is discussed in Section 2.2. After electroplating the mold was removed by repeating the two RIE steps (Fig. 2f).

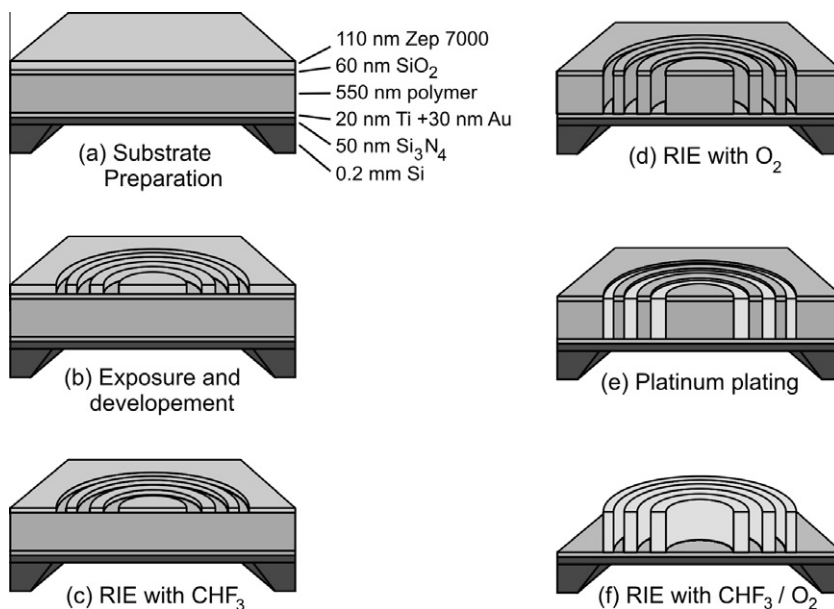


Fig. 2. The electroplating-based platinum zone plate fabrication process.

**Table 1**

Summary of the parameters for the platinum electroplating bath.

	Original bath	Modified bath
H <sub>2</sub> Pt(OH) <sub>6</sub>	20 g/l	20 g/l
KOH	15 g/l	9 g/l
Temperature	75 °C	60 °C
Current density	0.75 A/dm <sup>2</sup>	0.1 A/dm <sup>2</sup>
Anode	Pt-plated Ti	Pt-plated Ti

## 2.2. Platinum electroplating

Electroplating of Pt can be made from different complexes. Refs. [11,12] review the most common plating bath compositions. For this work we chose a modified hexahydroxyplatonic (H<sub>2</sub>Pt(OH)<sub>6</sub>) based solution proposed in Ref. [12]. Table 1 summarizes the bath parameters in its original and our modified form. During the initial experiments it was found that the plating mold could separate from the substrate if the plating did not start immediately or if the plating rate was too low. Reducing the potassium hydroxide concentration (KOH) to 9 g/l, thereby lowering the pH to 9.6, and decreasing the temperature lead to a more sustainable mold without a deterioration of the quality of the plated metal.

For the nanofabrication experiments only a small volume of solution was prepared at the time. A solution of 200 mg of H<sub>2</sub>Pt(OH)<sub>6</sub> and 90 mg of KOH in 10 ml of distilled water was prepared in the following way. The bath components were first dissolved in 20 ml of water by stirring and heating at 90 °C for 1 h. During this time the solution evaporated to the volume of 10 ml. No precipitation was observed. In the case of extra evaporation the volume was adjusted to 10 ml by adding distilled water. Then the solution was cooled to room temperature and filtered.

During operation the bath was heated to 60 °C and constantly stirred. A platinum plated Ti rod was used as anode. A cover ensured minimum evaporation of water. The plating was done with direct current with a current density of 0.1 A/dm<sup>2</sup>. This resulted in a plating rate of ~20 nm/min. The bath could be used over days without any noticeable deterioration in quality of the plated nanostructures. However, due to the small bath volume and repeated immersion of new samples that contaminates and removes a small amount of solution, the bath is routinely changed after plating ~10 samples.

## 3. Results and discussion

The process was evaluated by inspection of the electroplated structures and zone plates in the scanning electron microscope (SEM) and also by diffraction efficiency measurements at the European Synchrotron Radiation Facility (ESRF) [19].

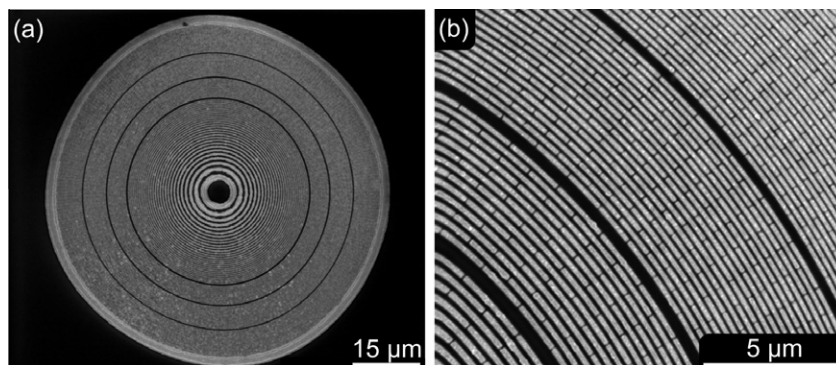


**Fig. 3.** SEM images of a fabricated Pt zone plate. The zone plate has a  $dr_N$  of 100 nm and has a thickness of 550 nm.

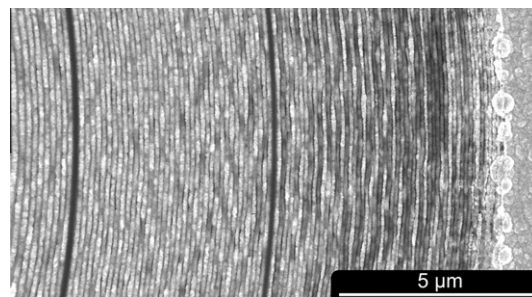


**Fig. 4.** SEM image of a Pt zone plate with  $dr_N = 50$  nm and a thickness of 530 nm. The high aspect ratio caused tilting in the outermost zones.

### 3.1. Fabricated zone plates optics

Pt zone plates with 100 and 50 nm outermost zones were fabricated. Fig. 3 shows a SEM image of a  $dr_N = 100$  nm zone plate with a diameter of 75 μm and a thickness of 550 nm. In (a) an overview of the full zone plate is shown and (b) depicts a close up of the outer part. The whole zone plate pattern is of the same quality. The plated Pt has uniformly filled the mold. To increase the rigidity of the plating mold, support bars were added to the design, which results in the brick pattern of the plated Pt. The three rings were also added to avoid the domino effect of collapsing that can occur if the zones start to tilt at a certain location.

To test the limit of the present process,  $dr_N = 50$  nm zone plates were also fabricated. Fig. 4 shows the outermost part such zone plate with a diameter of 75 μm and a thickness of 530 nm. The pattern looks excellent until the outer support ring but after that, where  $dr_N$  is between 60 and 50 nm, the pattern is slightly distorted. This is a result partly due to the high aspect ratio (10.6:1) but also an effect of longer O<sub>2</sub>-etch of the polyimide mold. The O<sub>2</sub> etching of the polyimide is aspect ratio dependent. To ensure a clearing of the outermost narrow zones the etch time must be increased ~50% for the 50-nm compared to the 100-nm zone plates. This results in increased lateral hard mask erosion and thereby a thinner and more fragile mold. For the zone plate in Fig. 4, the erosion has also completely removed the support bar structure. In Fig. 5(a) the quality of 50 nm structures is demonstrated by a result from plating in a lower mold. The image shows a grating with 50 nm half period and a height of 300 nm. In future work the SiO<sub>2</sub> hard mask thickness will be increased to allow for higher aspect ratios.

### 3.2. Efficiency measurements

To test the performance of the fabricated zone plates we measured the diffraction efficiencies at 8 keV X-ray energy. The measurements were performed at the ID06 beamline at ESRF.

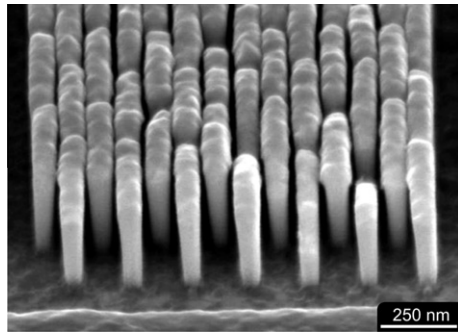


**Fig. 5.** SEM image of a 50 nm width platinum plated grating structures with the height of 300 nm.

**Table 2**  
Efficiency measurements of 4 Pt zone plates.

	drN (nm)	Thickness	Theoretical eff. (%)	Measured eff. (%)
Zone plate 1	100	600	11.7	7.7
Zone plate 2	100	580	11.1	8.2
Zone plate 3	50	570	10.8	5.5
Zone plate 4	50	590	11.3	4.6

Detuning of the monochromator ensured that the contributions from higher undulator orders to the X-ray beam were kept to a minimum. A homogeneous part of the beam was defined by a 100  $\mu\text{m}$  diameter pinhole and the zone plate was placed downstream. The intensity in the first order focus was measured by scanning a 10  $\mu\text{m}$  pinhole across the focus and recording the transmitted intensity with a diode. The contributions from other zone plate diffraction orders were removed by correcting the intensity in the focus with the intensity just to the side of it. After this, the zone plate and 10  $\mu\text{m}$  pinhole was removed and the reference intensity incident through the 100  $\mu\text{m}$  pinhole was measured. The ratio between the first-order focus intensity and the reference intensity, corrected for higher-order contributions and current variations in the stored electron beam, gives the diffraction efficiency. Table 2 shows the measured diffraction efficiencies for four different zone plates. The table also includes the thickness of the zone plates and the calculated theoretical efficiency for each zone plate. The theoretical efficiency is corrected for the efficiency loss from the fractional 10% area of the support structures as it was designed in the exposure file. The support structure appears smaller in Fig. 3(b) and is not visible in Fig. 4. This is due to an over etch of the hard mask, which has partly or totally removed the uppermost part of the support that is visible when imaging from above. The measured efficiencies are about 70% of the theoretical values for the 100 nm zone plates. This is about the same fraction of the theoretical value as we previously have obtained for soft X-ray nickel zone plates [20]. For the 50-nm zone plates about 50% of the theoretical value was measured. The main reason for the reduced efficiency is that the line-to-space ratio of the structures is not 1:1 over the whole zone plate. A further efficiency loss for the 50 nm

zone plates can be attributed to the fact that the smaller zones, from about 60 nm and onwards, are increasingly tilted.

#### 4. Conclusions

We have demonstrated platinum as a hard-X-ray zone plate material. The electro-plating-based fabrication process provides zone plates with high uniformity and the measured diffraction efficiency is 70% of the theoretical for 100 nm zone plates. The problems of obtaining high aspect ratio for <50 nm zones appears to be solvable. We plan to increase the hard mask thickness and improve the etch process to get a mold with better line-to-space ratio and profile. Platinum therefore appears to be an attractive alternative to, e.g., Au zone plates due to the higher diffraction efficiency of Pt in the 5–12 kV range and its higher melting point and, thus, better resistance to high-temperature operation. In addition, the nanostructure properties of Pt show promise for multi-material hard X-ray zone plates.

#### Acknowledgements

The authors gratefully acknowledge the financial support of the Swedish Strategic Research Foundation, the Göran Gustafsson Foundation, and Wallenberg Foundation. The research leading to these results has also received funding from the European Community's Seventh Framework Programme (FP7/2007-2013) under grant agreement No. 226716. Thanks also to Ray Barrett at the ESRF.

#### References

- [1] F. Nolting, C. David, F. Pfeiffer, C. Quitmann, M. Stampanoni (Eds.), in: Ninth International Conf. on X-ray Microscopy, J. Physics: Conf. Series 186, 2009.
- [2] D.T. Attwood, *Soft X-Rays and Extreme Ultraviolet Radiation*, Cambridge University Press, Cambridge, 1999.
- [3] A. Osawa, T. Tamamura, T. Ishii, H. Yoshihara, T. Kagoshima, *Microelectron. Eng.* 35 (1997) 525.
- [4] P. Charalambous, X-ray microscopy, in: T. Warwick, W. Meyer-Ilse, D. Attwood (Eds.), *AIP Conf. Proceedings*, vol. 507, 2007, p. 625.
- [5] J. Vila-Comamala, K. Jefimovs, J. Raabe, T. Pilvi, R.H. Fink, M. Senoner, A. Maaßdorf, M. Ritala, C. David, *Ultramicroscopy* 109 (2009) 1360.
- [6] J. Vila-Comamala, S. Gorelick, E. Färm, C.M. Kewish, A. Diaz, Ray Barret, V.A. Guzenko, M. Ritala, C. David, *Optics Express* 19 (2010) 175.
- [7] Y. Feng, M. Feser, A. Lyon, S. Rishton, X. Zeng, S. Chen, S. Sassolini, W. Yun, *J. Vac. Sci. Technol. B* 25 (2007) 2004.
- [8] J. Reinspach, M. Lindblom, O.v. Hofsten, M. Bertilson, H.M. Hertz, A. Holmberg, *J. Vac. Sci. Technol. B* 27 (2009) 2593.
- [9] D. Nilsson, A. Holmberg, H. Sinn, U. Vogt, *Nucl. Instrum. Methods A* 621 (2010) 620.
- [10] M. Lindblom, J. Reinspach, O.v. Hofsten, M. Bertilson, H.M. Hertz, A. Holmberg, *J. Vac. Sci. Technol. B* 27 (2009) L5.
- [11] C.R.K. Rao, D.C. Trivedi, *Coordination Chem. Rev.* 249 (2005) 613.
- [12] M.E. Baumgärtner, C.J. Raub, *Platinum Metals Rev.* 32 (1988) 188–197. and references therein.
- [13] C. Xiang, M.A. Thompson, F. Yang, E.J. Menke, L.-M.C. Yang, R.M. Penner, *Phys. Stat. Sol. C* 5 (2008) 3503.
- [14] A.P. Suryavanshi, M.F. Yu, *Nanotechnology* 18 (2007) 05305.
- [15] H.K. Seo, D.J. Park, J.Y. Park, *IEEE Sensors J.* 7 (2007) 945.
- [16] C. de Haro, R. Mas, G. Abadal, J. Muñoz, F. Perez-Murano, C. Dominguez, *Biomaterials* 23 (2002) 4515.
- [17] T. Kikuchi, H. Takahashi, T. Maruko, *Electrochimica Acta* 52 (2007) 2352.
- [18] A. Holmberg, S. Rehbein, H.M. Hertz, *Microel. Eng.* 73–74 (2004) 639.
- [19] [www.esrf.fr](http://www.esrf.fr).
- [20] M. Bertilson, P.A.C. Takman, U. Vogt, A. Holmberg, H.M. Hertz, *Rev. Sci. Instrum.* 78 (2007) 026103–026113.